The low temperature magnetostructural transition in $Pr_{0.50}Sr_{0.50}CoO_3$: Bulk versus thin film behavior

J. Padilla-Pantoja,[1] J. Herrero-Martín,[2] X. Torrelles,[1] B. Bozzo,[1] J. Blasco,[3] C. Ritter,[4] and J. L. García-Muñoz[1,a)]
[1]*Institut de Ciència de Materials de Barcelona, ICMAB-CSIC, Campus Univ. de Bellaterra, E-08193 Bellaterra, Spain*
[2]*ALBA Synchrotron Light Source, 08290 Cerdanyola del Vallès, Barcelona, Spain*
[3]*Instituto de Ciencia de Materiales de Aragón, CSIC-Univ. de Zaragoza, 50009 Zaragoza, Spain*
[4]*Institute Laue Langevin, BP 156, 38042 Grenoble Cedex 9, France*

(Presented 8 November 2013; received 23 September 2013; accepted 7 November 2013; published online 26 February 2014)

We present a comparative study of the magnetic transitions in metallic $Pr_{0.50}Sr_{0.50}CoO_3$ (PSCO) perovskites prepared in polycrystalline and thin film forms. As the bulk system, the strained epitaxial PSCO (010) film grown on LAO (100) is metallic in all the temperature range, with a ferromagnetic transition at 225 K, close to $T_c \sim 235$ K in the ceramic PSCO specimen. Unlike the bulk system, the PSCO film does not show the second magnetic transition on cooling. In the ceramic sample, the second magnetic transition is coupled to an orthorhombic-to-monoclinic symmetry change. There is a contraction of the average ⟨Pr-O⟩ bond distance in the monoclinic phase below T_a, but the ⟨Co-O⟩ bond length is not modified across the transition. The orthorhombic to monoclinic structural transition stabilizes four short Pr-O2 bonds to basal oxygens in CoO_6 octahedra. A strong hybridization of Pr 4*f* and O 2*p* orbitals in these bonds can be activated at T_a and probably assist the magnetostructural transition. © *2014 AIP Publishing LLC*. [http://dx.doi.org/10.1063/1.4865465]

I. INTRODUCTION

The properties of $Pr_{0.50}Ca_{0.50}CoO_3$ (PCCO) and $Pr_{0.50}Sr_{0.50}CoO_3$ (PSCO) perovskites are a very good example of the interesting phenomena in structurally simple cobalt oxides with spin-charge-lattice coupling. $Pr_{0.5}Ca_{0.5}CoO_3$ exhibits a non-conventional metal-insulator and Co spin-state transition at $T_{MI} \sim 80$ K where the insulating state is stabilized by electron transfer from Pr to Co sites.[1–3]This exceptional electronic mechanism in PCCO and other $(Pr,Ln)_{1-x}Ca_xCoO_3$ cobaltites (*Ln*: lanthanide) with *Pnma* symmetry is based on the contraction of selected Pr-O bonds[1] that generate a first-order Pr^{3+} to Pr^{4+} valence transition at T_{mi}. This is accompanied by the stabilization of the Co^{3+}LS state.[1–3]

Metallic $Pr_{0.50}Sr_{0.50}CoO_3$ presents *Imma* symmetry and anomalous magnetic properties.[4–6] It becomes ferromagnetic (FM) below $T_C = 230$ K, but a second transition at $T_a \sim 120$ K produces an unusual step-like behavior of the magnetization and presumably a change of the magnetic easy axis.[3] This unexpected second magnetic transition in FM/metallic PSCO has been ascribed to a coupling of structural and magnetocrystalline anisotropy instabilities.[6] However, a convincing detailed explanation, which must account for some intriguing observations, is still pending. Among them, (i) the hysteretic sharp decrease in the magnetization at low fields at T_a; (ii) the anomalous H dependence of M(T), which increases at the transition on cooling at higher fields; (iii) the absence of the second transition in other half-doped cobaltites without Pr ions, which suggests the importance of this ion. So, the transition was shown to progressively disappear as Pr is replaced by La in $(La_{1-y}Pr_y)_{0.5}Sr_{0.5}CoO_3$ and does not occur in $Nd_{0.5}Sr_{0.5}CoO_3$;[6] and (iv) The evidence of sudden structural changes and the observation of new structural reflections at $T < T_a$ opened the possibility to the occurrence of an orbital or charge order, and seems to be at the origin of changes in the magnetocrystalline anisotropy of this perovskite. Troyanchuk *et al.*[5] and later Leighton *et al.*,[6] using different structural descriptions for the low temperature phase, underlined the possible importance of the Pr 4*f* – O 2*p* hybridization for this transition.

II. EXPERIMENT

Polycrystalline samples of $Pr_{0.50}Sr_{0.50}CoO_3$ were prepared following standard solid-state reaction methods, from the intimate mixture of high purity precursor oxides (Co_3O_4 and Pr_6O_{11} and $SrCO_3$). The final sintering temperature was 1170 °C, under oxygen atmosphere. Samples were then slowly cooled down to room temperature in the presence of oxygen. In addition, thin $Pr_{0.50}Sr_{0.50}CoO_3$ films (70 nm) were grown on (100)-oriented $LaAlO_3$ (LAO) single-crystal substrates ($3 \times 5 \times 1$ mm^3) by RHEED assisted Pulsed Laser Deposition technique by using a KrF excimer laser at energies of 65 mJ and a fluence of 1.4 J/cm^2, and stoichiometric PSCO ceramic dense pellet as a target. After exploring different growth and annealing conditions, strained epitaxial PSCO (010) film was grown at 700 °C under 0.40 mbar O_2 partial pressure. An annealing was done at 500 °C for 1 h under 400 mbar O_2 pressure, followed by a slow cooling from 500 °C to room temperature (RT). Sample characterization included conventional dc magnetometry and transport measurements, and x-ray and neutron diffraction.

a)Author to whom correspondence should be addressed. Electronic mail: garcia.munoz@icmab.es.

Polycrystalline samples were tested with x-ray powder diffraction using a Siemens D-5000 diffractometer, and found to be single phase. Neutron powder diffraction (NPD) experiments at the Institute Laue-Langevin (Grenoble) were performed using D20 diffractometer ($\lambda = 1.87$ Å) in the temperature range between 15 and 250 K. The structure of the film was studied at the surface diffraction beamline BM25B at the ESRF (Grenoble), using a one dimensional detector (NaI scintillator).

III. RESULTS AND DISCUSSION

The x-ray diffraction (XRD) scans confirmed an epitaxial growth of the PSCO film, with the longest axis ($2a_c$) of the perovskite structure perpendicular to the surface. Four-fold symmetry was shown by azimuthal (Phi) scans. In addition, the PSCO film was mounted in a cryogenically adapted UHV baby chamber coupled to a six-circle diffractometer in BM25B. The incident beam energy was set to 15.0 keV. The (H,K,L) indices of the measured reflections are defined in the cubic basis of the LAO substrate ($a_{LAO} = 3.79$ Å). The PSCO film grows with their in-plane lattice parameters identical and rotated 45° respect to the LaO (100) substrate ($a_f = c_f = \sqrt{2}*a_{LAO} = 5.35$ Å) with an out-of plane lattice parameter close to that of the long PSCO bulk lattice value, $b_f = 7.71$ Å (bulk value 7.60 Å). Varying the incident beam angles, diffraction patterns showed uniform lattice parameters in the z direction, suggesting a strained 2D-like growth. Selected synchrotron x-ray diffraction scans of the PSCO epitaxial film at RT are shown in Figure 1. In Ref. 7, the reflections labelled by letters are described in the basis of the film. Reflections in Fig. 1(a) ($h+k+l = 2n$) are compatible with both *Pnma* and *Imma* symmetries. Reflections of "d" and "e" type ($h+k+l = 2n+1$), permitted by *Pnma* symmetry and forbidden by *Imma*, are absent in the scans shown in Figs. 1(b) and 1(c). Thus, Bragg reflections conditions in the film exclude the *Pnma* symmetry, and agree with the *Imma* space group, with the glide plane perpendicular to the surface. The mismatch of the LAO substrate induces an in-plane compressive strain into the PSCO film with respect to the bulk (−1.1%); and a tensile strain (+1.3%) along the out-of-plane direction (b_f).

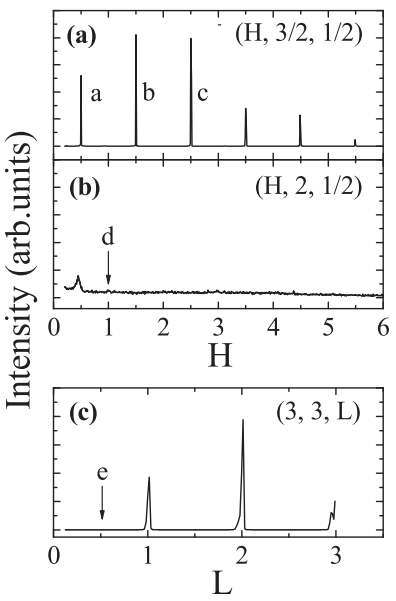

FIG. 1. Selected synchrotron x-ray diffraction reciprocal space scans at RT from PSCO epitaxial film (see explanation in the text and Ref. 7).

Figure 2 shows the magnetic susceptibility of the PSCO film as a function of temperature. The resistivity curve is shown in the inset. They are compared with the behaviour of the ceramic sample. Similarly, as for bulk PSCO, the film is metallic down to the lowest temperature. Both samples are ferromagnetic below $T_c \sim 235$ K (ceramic) and ~225 K (film) (measured under H = 100 Oe). Despite the Curie temperature is rather similar and both specimens are metallic, their low temperature behaviour is markedly different. On cooling, the ceramic PSCO ceramic shows a notable reduction of the FM moment (step in the magnetization) at about 120 K. NPD data confirm a structural transition from orthorhombic to monoclinic symmetry (*Imma* to *I2/a*) at this temperature. However, this second transition has been suppressed in the epitaxial PSCO film. No anomalies were detected at low temperatures in the magnetization (black filled dots in Fig. 2) or the crystal symmetry of the film by synchrotron x-ray surface diffraction.

NPD patterns from polycrystalline PSCO were satisfactorily refined using *Imma* ($\chi^2 = 1.40$) and *I2/a* ($\chi^2 = 1.66$) symmetries, respectively, above and below the magneto-structural transition at $T_A \sim 120$ K. Besides a reduction of the FM ordered moment (from 1.6 to 0.9 μ_B/Co), the observed cell transformation agrees with the evolution of cell parameters reported in Ref. 6. A full description of the low temperature phase and a more detailed analysis of the transformation will be published elsewhere. Here, we wish to draw the attention on the different role of Pr-O and Co-O bonds (Fig. 3). From Rietveld analysis of NPD data collected as a function of temperature, we have extracted the temperature evolution of the average R-O and Co-O bond-lengths across the transition at T_a. Their evolution across T_a, plotted in Figure 3, is rather similar to $Pr_{0.50}Ca_{0.50}CoO_3$ across T_{MI}[1]: the Co-O distance hardly changes across the second magnetic transition; however, the average ⟨(Pr,Sr)-O⟩ bond length exhibits a sudden contraction at T_a on cooling ($\langle(Pr,Sr)\text{-}O\rangle^{XII} \sim -0.5\%$, or $\langle(Pr,Sr)\text{-}O\rangle^{VIII} \sim -4\%$ if only

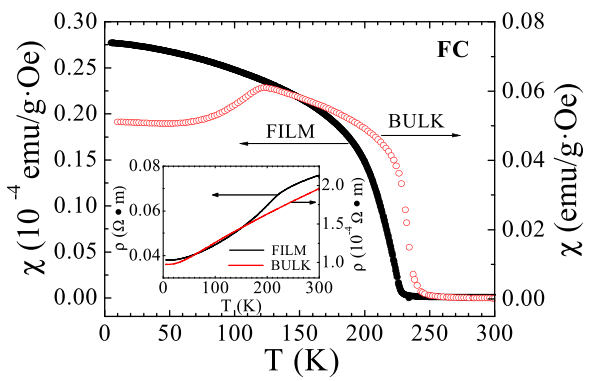

FIG. 2. Magnetic susceptibility of the PSCO film (left axis) and the PSCO ceramic sample (right axis). Field-cooled curves measured on heating under 100 Oe. The inset shows the metallic zero-field resistivity as a function of temperature in both samples.

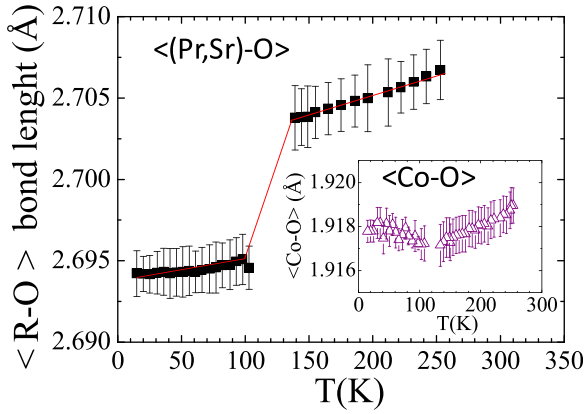

FIG. 3. Evolution the average (Pr,Sr)-O bond distance (XII-coord.) in bulk PSCO across the second magnetic transition at T_a. The solid lines are guides to the eye. The inset shows the evolution of the average Co-O bond distance in the CoO_6 octahedra.

the first eight oxygens in the nearest neighbor shell around R-site is considered).[8]

In the monoclinic phase of PSCO, the four shortest R-O bondlengths are (Pr,Sr)-O2 = 2.494(5) and 2.546(5) Å (both of them double), indicating a probable strong hybridization of Pr 4*f* and O 2 *p* orbitals. Completing the first coordination shell, the following four shortest R-O distances below T_a are 2.65, 2.67 and two bondlengths of 2.70 Å (all four bonds of (Pr,Sr)-O1 type). As usually, we used labels O1 and O2 referred to, respectively, apical and basal oxygens in CoO_6 octahedra. Therefore, the orthorhombic to monoclinic structural transition stabilizes four short Pr-O2 bonds to basal oxygens in CoO_6 octahedra, giving strong support to the active participation of 4*f* electrons of Pr in the atypical magnetostructural changes of $Pr_{0.50}Sr_{0.50}CoO_3$.

IV. CONCLUSION

In summary, the formation of four short Pr-O2 bonds to oxygens in the basal plane of the CoO_6 octahedra below T_a strongly suggests an active participation of Pr 4*f* electrons in the anomalous transition of $Pr_{0.50}Sr_{0.50}CoO_3$. These results emphasize the need for further experiments (like x-ray absorption studies at Pr edges) to confirm and clarify the role of Pr 4*f*-O 2*p* orbital hybridization effects on this transition. The suppression of the transition in metallic PSCO (010) films epitaxially grown on LAO (100), with very similar Curie temperature, evidences the relevance of the lattice degrees of freedom for the magnetostructural changes in bulk PSCO samples.

ACKNOWLEDGMENTS

We thank financial support from MICINN (Spanish government) under Projects MAT2009-09308, MAT2012-38213-C02-02, and CSD2007-00041 (NANOSELECT), and the ILL for granting beamtime. J.P-P thanks CSIC for JAE-Pre contract. We acknowledge the ESRF and the staff of BM25 beamline for technical assistance.

[1]A. J. Barón-González, C. Frontera, J. L. García-Muñoz, J. Blasco, and C. Ritter, Phys. Rev. B **81**, 054427 (2010); J. L. García-Muñoz, C. Frontera, A. J. Barón-González, S. Valencia, J. Blasco, R. Feyerherm, E. Dudzik, R. Abrudan, and F. Radu, Phys. Rev. B **84**, 045104 (2011).
[2]J. Hejtmánek, E. Šantava, K. Knížek, M. Maryško, Z. Jirák, T. Naito, H. Sasaki, and H. Fujishiro, Phys. Rev. B **82**, 165107 (2010); K. Knizek, J. Hetjmánek, P. Novák, and Z. Jirák, Phys. Rev. B **81**, 155113 (2010).
[3]J. Herrero-Martín, J. L. García-Muñoz, S. Valencia, C. Frontera, J. Blasco, A. J. Barón-González, G. Subías, R. Abrudan, F. Radu, E. Dudzik, and R. Feyerherm, Phys. Rev. B **84**, 115131 (2011); Phys. Rev. B **86**, 125106 (2012).
[4]R. Mahendiran and P. Schiffer, Phys. Rev. B **68**, 024427 (2003).
[5]I. O. Troyanchuk, D. V. Karpinskii, A. N. Chobot, D. G. Voitsekhovich, and V. M. Bobryanskii, JETP Lett. **84**, 151 (2006); A. M. Balagurov, I. A. Bobrikov, D. V. Karpinsky, I. O. Troyanchuk, V. Y. Pomjakushin, and D. V. Sheptyakov, JETP Lett. **88**, 531 (2008).
[6]C. Leighton, D. D. Stauffer, Q. Huang, Y. Ren, S. El-Khatib, M. A. Torija, J. Wu, J. W. Lynn, L. Wang, N. A. Frey, H. Srikanth, J. E. Davies, K. Liu, and J. F. Mitchell, Phys. Rev. B **79**, 214420 (2009); N. A. Frey Huls, N. S. Bingham, M. H. Phan, H. Srikanth, D. D. Stauffer, and C. Leighton, Phys. Rev. B **83**, 024406 (2011).
[7]Selected (h,k,l) reflections in Figure 1, defined in the basis of the PSCO film, correspond to: a = (−1,1, 2), b = (0,1,3), c = (1,1,4), d = (−1,1,3), and e = (0,1,6).
[8]The coordination polyhedron around R atoms is composed of 12 oxygen atoms (8+4). As in many perovskite structures, the R-O distances to the last four oxygens in the coordination polyhedron are sensibly longer. The average ⟨R-O⟩ distance is sometimes calculated considering only the first 8 oxygen neighbors.